

Factorization and Criticality in Finite XXZ Systems of Arbitrary Spin

M. Cerezo,¹ R. Rossignoli,^{1,2} N. Canosa,¹ and E. Ríos³

¹*Instituto de Física de La Plata, CONICET, and Departamento de Física, Universidad Nacional de La Plata, C.C. 67, La Plata 1900, Argentina*

²*Comisión de Investigaciones Científicas de la Provincia de Buenos Aires (CIC), La Plata 1900, Argentina*

³*Departamento de Ingeniería Química, Universidad Tecnológica Nacional, Facultad Regional Avellaneda, C.C. 1874, Argentina*

(Received 17 July 2017; revised manuscript received 19 September 2017; published 1 December 2017)

We analyze ground state (GS) factorization in general arrays of spins s_i with XXZ couplings immersed in nonuniform fields. It is shown that an exceptionally degenerate set of completely separable symmetry-breaking GSs can arise for a wide range of field configurations, at a quantum critical point where all GS magnetization plateaus merge. Such configurations include alternating fields as well as zero-bulk field solutions with edge fields only and intermediate solutions with zero field at specific sites, valid for d -dimensional arrays. The definite magnetization-projected GSs at factorization can be analytically determined and depend only on the exchange anisotropies, exhibiting critical entanglement properties. We also show that some factorization-compatible field configurations may result in field-induced frustration and nontrivial behavior at strong fields.

DOI: 10.1103/PhysRevLett.119.220605

One of the most remarkable phenomena arising in finite interacting spin systems is that of factorization. For particular values and orientations of the applied magnetic fields, the system possesses a completely separable exact ground state (GS) despite the strong couplings existing between the spins. The close relation between GS factorization and quantum phase transitions was first reported in Ref. [1] and has since been studied in various spin models [2–12], with general conditions for factorization discussed in Refs. [7,13]. Aside from some well-known integrable cases [14–17], higher-dimensional systems of arbitrary spin in general magnetic fields are not exactly solvable, so that exact factorization points and curves provide a useful insight into their GS structure.

The XXZ model is an archetypal quantum spin system which has been widely studied to understand the properties of interacting many-body systems and their quantum phase transitions [18–23]. It can emerge as an effective Hamiltonian in different scenarios, like bosonic and fermionic Hubbard models [24–27] and interacting atoms in a trapping potential [27–29]. Renewed interest in it has been enhanced by the recent advances in quantum control with state-of-the-art technologies [30,31], which enable its finite size simulation even with tunable couplings and fields in systems such as cold atoms in optical lattices [27–29, 32–34], photon-coupled microcavities [35–37], superconducting Josephson junctions [38–42], trapped ions [30, 43–46], atoms on surfaces [47], and quantum dots [48]. These features make it a suitable candidate for implementing quantum information processing tasks [27–31,48–55].

Our aim here is to show that, in finite XXZ systems of arbitrary spin under nonuniform fields, highly degenerate exactly separable symmetry-breaking GSs can arise

for a wide range of field configurations in arrays of any dimension, at an outstanding critical point where all magnetization plateaus merge and entanglement reaches full range. The Pokrovsky-Talapov (PT)-type transition in a spin-1/2 chain in an alternating field [20] is shown to correspond to this factorization. Magnetization phase diagrams, showing nontrivial behavior at strong fields, and pair entanglement profiles for distinct factorization-compatible field configurations are presented, together with analytic results for definite magnetization GSs.

We consider an array of N spins s_i interacting through XXZ couplings and immersed in a general nonuniform magnetic field along the z axis. The Hamiltonian reads

$$H = -\sum_i h^i S_i^z - \sum_{i<j} J^{ij} (S_i^x S_j^x + S_i^y S_j^y) + J_z^{ij} S_i^z S_j^z, \quad (1)$$

with h^i and S_i^μ the field and spin components, respectively, at site i and J^{ij} and J_z^{ij} the exchange coupling strengths. Since H commutes with the total spin component $S^z = \sum_i S_i^z$, its eigenstates can be characterized by their total magnetization M along z . The exact GS will then exhibit definite M plateaus as the fields h^i are varied, becoming maximally aligned ($|M| = S \equiv \sum_i s_i$) and hence completely separable for sufficiently strong uniform fields. Otherwise, it will be normally entangled.

We now investigate the possibility of H having a nontrivial completely separable GS of the form

$$|\Theta\rangle = \otimes_{i=1}^N e^{-i\phi_i S_i^z} e^{-i\theta_i S_i^y} |\uparrow_i\rangle = |\nearrow \swarrow \searrow \dots\rangle, \quad (2)$$

where the local state $|\uparrow_i\rangle$ ($S_i^z |\uparrow_i\rangle = s_i |\uparrow_i\rangle$) is rotated to an arbitrary direction $\mathbf{n}_i = (\sin \theta_i \cos \phi_i, \sin \theta_i \sin \phi_i, \cos \theta_i)$.

$|\Theta\rangle$ will be an exact eigenstate of H iff two sets of conditions are met [13]. The first ones,

$$J^{ij} \cos \phi_{ij} (1 - \cos \theta_i \cos \theta_j) = J_z^{ij} \sin \theta_i \sin \theta_j, \quad (3)$$

$$J^{ij} \sin \phi_{ij} (\cos \theta_i - \cos \theta_j) = 0, \quad (4)$$

where $\phi_{ij} = \phi_i - \phi_j$, are field independent and relate the alignment directions with the exchange couplings, ensuring that H does not connect $|\Theta\rangle$ with two-spin excitations. The second ones,

$$h^i \sin \theta_i = \sum_{j \neq i} s_j [J^{ij} \cos \phi_{ij} \cos \theta_i \sin \theta_j - J_z^{ij} \sin \theta_i \cos \theta_j], \quad (5)$$

$$0 = \sum_{j \neq i} s_j J^{ij} \sin \phi_{ij} \sin \theta_j, \quad (6)$$

determine the factorizing fields (FFs) and cancel all elements connecting $|\Theta\rangle$ with single spin excitations, representing the mean field equations $\partial_{\theta_i(\phi_i)} \langle \Theta | H | \Theta \rangle = 0$.

These equations are always fulfilled by aligned states ($\theta_i = 0$ or $\pi \forall i$). We now seek solutions with $\theta_i \neq 0, \pi$ and $\phi_{ij} = 0 \forall i, j$ [56]. Equations (4) and (6) are then trivially satisfied, whereas Eq. (3) implies

$$\eta_{ij} \equiv \frac{\tan(\theta_j/2)}{\tan(\theta_i/2)} = \Delta_{ij} \pm \sqrt{\Delta_{ij}^2 - 1}, \quad (7)$$

where $\Delta_{ij} = J_z^{ij}/J^{ij} = \Delta_{ji}$. Such solutions then become feasible if $|\Delta_{ij}| \geq 1$. For $|\Delta_{ij}| > 1$, (7) yields two possible values of θ_j for a given θ_i ($\theta_j = \vartheta_{\pm 1}$ if $\theta_i = \vartheta_0$; see Fig. 1, top left). And given $\theta_i, \theta_j \neq 0, \pi$, there is a single value $\Delta_{ij} = (\eta_{ij} + \eta_{ij}^{-1})/2$ satisfying (7) ($\eta_{ij}^{-1} = \Delta_{ij} \mp \sqrt{\Delta_{ij}^2 - 1}$).

If Eq. (7) is satisfied for all coupled pairs, Eq. (5) leads to the factorizing fields

$$h_s^i = \sum_j s_j \nu_{ij} J^{ij} \sqrt{\Delta_{ij}^2 - 1}, \quad (8)$$

where $\nu_{ij} = -\nu_{ji} = \pm 1$ is the sign in (7). These fields are independent of the angles θ_i and always fulfill the weighted zero sum condition

$$\sum_i s_i h_s^i = 0. \quad (9)$$

The ensuing energy $E_{\Theta} = -\sum_i s_i \mathbf{n}_i \cdot [\mathbf{h}_s^i + \sum_{j>i} \mathcal{J}^{ij} s_j \mathbf{n}_j]$ ($\mathcal{J}_{\mu\nu}^{ij} \equiv J_{\mu}^{ij} \delta_{\mu\nu}$) depends only on the strengths J_z^{ij} :

$$E_{\Theta} = -\sum_{i<j} s_i s_j J_z^{ij}, \quad (10)$$

coinciding with that of the $M = \pm S$ aligned states in such a field. It is proved (see Supplemental Material [57]) that, if $J_z^{ij} \geq 0 \forall i, j$, (10) is the GS energy of such H . Essentially, H can be written as a sum of pair Hamiltonians H^{ij} whose

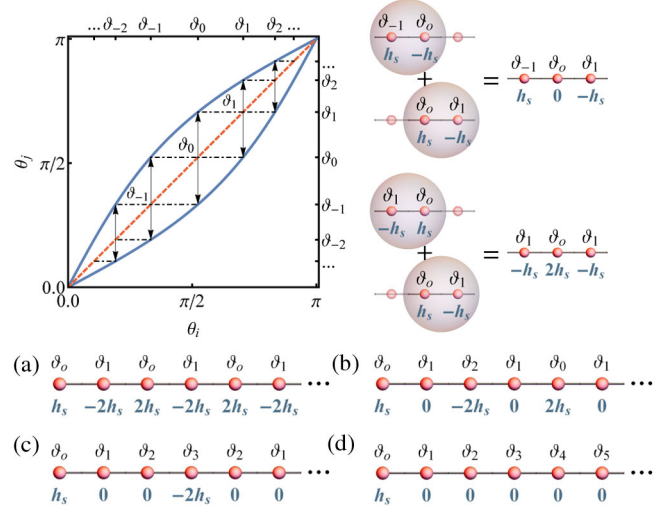


FIG. 1. Top left: The two solutions of Eq. (7) for θ_j vs θ_i (thick solid lines). For an arbitrary initial spin orientation ϑ_0 at one site, successive application of Eq. (7) determines the possible orientation angles (indicated by the arrows) of the remaining spins in a factorized eigenstate $|\Theta\rangle$. Each sequence of angles leads to a different factorizing field configuration determined by Eq. (8), shown in the top right panels for three spins and in the bottom rows for the first six spins of a chain with uniform spin and couplings. Two extremal cases arise: an alternating solution (a) and a zero-bulk field solution with edge fields only (d). Solutions with intermediate zero fields are also feasible (b),(c). In a cyclic chain, the first field is $2h_s$.

GS energies are precisely $-s_i s_j J_z^{ij}$. If $J_z^{ij} < 0 \forall i, j$, it is instead its highest eigenvalue.

These separable eigenstates do not have a definite magnetization, breaking the basic symmetry of H and containing components with all values of M . They can then arise only at an exceptional point where the GS becomes $2S + 1$ degenerate and all GS magnetizations plateaus coalesce: Since $[H, P_M] = 0$, with $P_M = (1/2\pi) \int_0^{2\pi} e^{i\varphi(S^z - M)} d\varphi$ the projector onto total magnetization M , $HP_M|\Theta\rangle = E_{\Theta}P_M|\Theta\rangle$ for all $M = -S, \dots, S$. All components of $|\Theta\rangle$ with definite M are exact eigenstates with the same energy (10). Moreover, the normalized projected states are independent of both ϕ and the seed angle $\theta_1 = \vartheta_0$, depending just on the exchange anisotropies Δ_{ij} and the signs ν_{ij} (see Supplemental Material [57]):

$$P_M|\Theta\rangle \propto \sum_{\substack{m_1, \dots, m_N \\ \sum_i m_i = M}} \left[\prod_{i=1}^N \sqrt{\binom{2s_i}{s_i - m_i}} \eta_{i,i+1}^{\sum_{j=1}^i m_j} \right] |m_1 \dots m_N\rangle, \quad (11)$$

where $\eta_{i,i+1}$ denote the ratios (7) along any curve in the array joining all coupled spins. In contrast with $|\Theta\rangle$, these states are entangled $\forall |M| \leq S - 1$ and represent the actual limit of the exact GS along the M th magnetization plateau as the factorization point is approached.

As a basic example, for a single spin- s pair with $J^{ij} = J$, GS factorization will arise whenever $J_z > 0$ and $|\Delta| = |J_z/J| > 1$, at opposite FFs $h_s^1 = -h_s^2 = \pm h_s$, with

$$h_s = sJ\sqrt{\Delta^2 - 1}. \quad (12)$$

At these points the GS is $4s + 1$ degenerate, with energy $E_\Theta = -s^2 J_z$ and projected GSs

$$\frac{P_M|\Theta\rangle}{\sqrt{\langle\Theta|P_M|\Theta\rangle}} = \sum_m \sqrt{\frac{\binom{2s}{s-m}\binom{2s}{s+m-M}}{Q_{2s-M}^{M,0}(\eta)}} \eta^{s+m-M} |m, M-m\rangle, \quad (13)$$

where $Q_n^{m,k}(\eta) = (\eta^2 - 1)^n P_n^{m-k, m+k}[(\eta^2 + 1)/(\eta^2 - 1)]$ with $P_n^{\alpha,\beta}(x)$ the Jacobi polynomials and η the ratio (7). These states are entangled, with (13) their Schmidt decomposition.

Spin chains.—The factorized GSs of a single pair can be used as building blocks for constructing separable GSs of a chain of N spins (Fig. 1). For first-neighbor couplings, after starting with a seed $\theta_1 = \vartheta_0 \in (0, \pi)$ at the first spin, $\theta_2, \dots, \theta_N$ are determined by Eq. (7). The two choices for θ_j at each step then lead to 2^{N-1} distinct factorized states and FF configurations in an open chain.

For uniform spins $s_i = s$ and couplings $J^{i,i+1} = J$, $\Delta_{i,i+1} = \Delta \forall i$, the FF (8) become $h_s^i = \nu_i h_s$, with h_s given by (12) and $\nu_i = \sum_j \nu_{ij} = \pm 2$ or 0 for bulk spins and ± 1 for edge spins. Among the plethora of factorizing spin and field configurations, two extremal cases stand out: a Néel-type configuration $\vartheta_0 \vartheta_1 \vartheta_0 \vartheta_1 \dots$, implying an alternating field $h_s^i = \pm 2(-1)^i h_s$ for bulk spins and $|h_s^1| = |h_s^N| = h_s$ for edge spins [Fig. 1(a)], and a solution with increasing angles $\vartheta_0, \vartheta_1, \vartheta_2, \dots$, implying a zero-bulk field and edge fields $h_s^1 = -h_s^N = \pm h_s$ [Fig. 1(d)]. Solutions with intermediate zero fields are also feasible [Figs. 1(b) and 1(c)]. In a cyclic chain ($N + 1 \equiv 1$, $J_\mu^{1N} = J_\mu$), the number of configurations is smaller, i.e., $\binom{N}{N/2} (\approx 2^{N-1}/\sqrt{\pi N/8})$ for large N , as (7) should be also fulfilled for the $1 - N$ pair, entailing $\theta_N = \vartheta_{\pm 1}$, N even, and an equal number of positive and negative choices in (7). For $\Delta \rightarrow 1$, $h_s \rightarrow 0$ and all solutions converge to a uniform $|\Theta\rangle$ [θ_i constant, Eq. (7)].

Spin lattices.—Previous arguments can be extended to d -dimensional spin arrays, like spin-star geometries [55] and square or cubic lattices with first-neighbor couplings and fixed $\Delta_{ij} = \Delta$. As the angles θ_j of all spins coupled to spin i should satisfy (7), they must differ from θ_i in just one step: $\theta_j = \vartheta_{k\pm 1}$ if $\theta_i = \vartheta_k$ (Fig. 1). Nonetheless, the number of feasible spin and field configurations still increases exponentially with lattice size (see Supplemental Material [57] for a detailed discussion). The FFs are $h_s^i = \pm \nu_i h_s$ with ν_i integer. In particular, the previous two extremal solutions remain feasible (see Fig. 4): By choosing in (7) alternating signs along rows, columns, etc., we obtain alternating FFs

$h_s^i = \pm 2d h_s$ for bulk spins [$h_s^{ij} = \pm 4(-1)^{i+j} h_s$ for $d = 2$], with smaller values at the borders. And by always choosing the same sign in (7), such that ϑ increases along rows, columns, etc., the FFs will be zero at all bulk spins, with nonzero fields $\nu_i h_s$ just at the border.

Definite M reduced states.—For uniform anisotropy Δ , all ratios $\eta_{i,i+1}$ in the projected states (11) will be either η or η^{-1} , and more explicit expressions can be obtained. For instance, for a spin- s array in an alternating FF, Eq. (11) leads, in any dimension, to just three distinct reduced pair states ρ_{ij}^M of spins $i \neq j$: ρ_{oe}^M (odd-even), ρ_{oo}^M , and ρ_{ee}^M , which will not depend on the actual separation between the spins, since $\rho_{i,j+k}^M = \rho_{i,j}^M \forall k$ even, due to the form of $|\Theta\rangle$. Their nonzero elements are

$$(\rho_{ij}^M)_{m_j, m'_j} = \eta^{f_{ij}} \frac{\sqrt{C_{m_j}^{s,m} C_{m'_j}^{s,m} Q_{Ns-2s-M+m}^{M, (\delta+2l_{ij})s}(\eta)}}{Q_{Ns-M}^{M, \delta s}(\eta)}, \quad (14)$$

where $m = m_i + m_j = m'_i + m'_j$ is the pair magnetization ($[\rho_{ij}^M, S_i^z + S_j^z] = 0$), $Q_n^{m,k}(\eta)$ was defined in (13), $C_k^{s,m} = \binom{2s}{s-k} \binom{2s}{s-m+k}$, and $f_{ij} = 2s - m_j - m'_j, 0, 4s - 2m, l_{ij} = 0, -1, 1$ for oe, oo, ee pairs, with $\delta = 0(1)$ for N even (odd). For $|M| < Ns$, these states are mixed (implying entanglement with the rest of the array) and also entangled for finite N , entailing that pair entanglement will reach full range, as discussed below.

Magnetic behavior.—The FFs (8) are critical points in the multidimensional field space (h^1, \dots, h^N) , as seen in Fig. 2 for a finite spin-1 cyclic chain in an alternating field (h_1, h_2, h_1, \dots) . While a large part of the field plane (h_1, h_2) corresponds for $\Delta > 1$ to an aligned GS ($M = \pm Ns$),

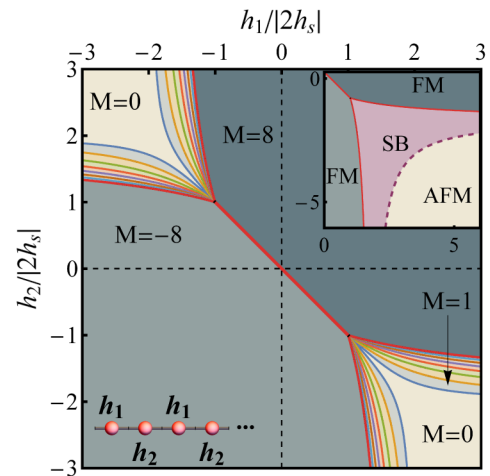


FIG. 2. GS magnetization diagram for alternating fields $h^{2i-1} = h_1$, $h^{2i} = h_2$ in an $N = 8$ spin-1 XXZ chain with $\Delta = 1.2$. All magnetization plateaus $M = Ns, \dots, -Ns$ coalesce at the factorizing fields $h_1 = -h_2 = \pm 2h_s$. The inset indicates the mean field (MF) phases.

sectors with GS magnetizations $|M| < Ns$ emerge precisely at the FFs $h_1 = -h_2 = \pm 2h_s$. These fields coincide with those of the PT-type transition for $h_1 = -h_2$ in a spin-1/2 chain [20], which then corresponds to the present GS factorization (holding for any spin s). The border of the aligned sector is actually determined by the hyperbola branches

$$\left(\frac{h_1}{2sJ} \pm \Delta\right) \left(\frac{h_2}{2sJ} \pm \Delta\right) = 1, \quad (15)$$

(for $|h_i| > 2h_s$, $\mp h_i/2sJ < \Delta$; see Supplemental Material [57]), which cross at the FF if $\Delta \geq 1$. Equation (15) also determines the onset of the symmetry-breaking (SB) MF solution (inset in Fig. 2), which ends in an antiferromagnetic (AFM) phase for strong fields of opposite sign (see [57] for more details).

Along lines $h_2 = h_1 + \delta$, the exact GS for $\Delta > 1$ then undergoes a single $-Ns \rightarrow Ns$ transition if $\delta < |4h_s|$ but $2Ns$ transitions $M \rightarrow M + 1$ if $|\delta| > 4h_s$, starting at the border (15). Hence, at factorization, the application of further fields $(\delta h_1, \delta h_2) = \delta h(\cos \gamma, \sin \gamma)$ enables us to select any magnetization plateau, which initially emerge at straight lines at angles $\tan \gamma_M = [(\langle S_1^z \rangle_M - \langle S_1^z \rangle_{M-1}) / (\langle S_2^z \rangle_{M-1} - \langle S_2^z \rangle_M)]$ [61]. Moreover, at this point an additional arbitrarily oriented local field \mathbf{h}^i applied at site i will bring down a single separable GS (that with $\mathbf{n}_i \parallel \mathbf{h}^i$), splitting the $2Ns + 1$ degeneracy and enabling a separable GS engineering [57].

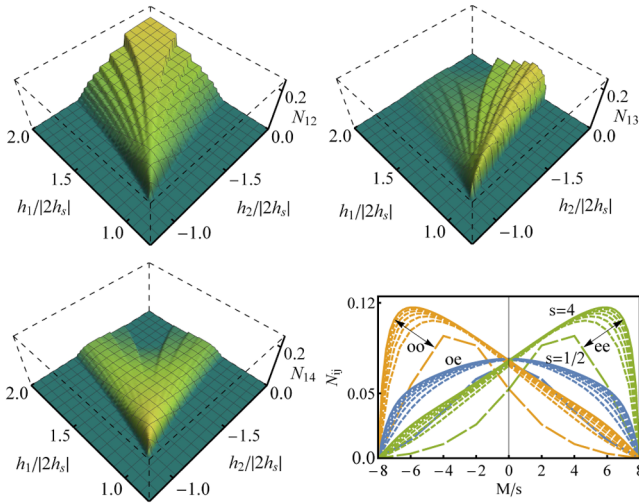


FIG. 3. Exact pair negativities N_{ij} between spins i and j in the exact GS of the spin-1 chain in Fig. 2, for fields h_1, h_2 of opposite sign and first (top left), second (top right), and third (bottom left) neighbors. Bottom right: The exact pair negativities at factorization ($h_1 = -h_2 = 2h_s$) in the definite magnetization GSs, for identical $N = 8$ spin- s chains with $s = 1/2, \dots, 4$. At this point there are just three distinct pair negativities: N_{oe} (odd-even), N_{oo} , and N_{ee} , independent of the actual separation $|i - j|$ and dependent on M .

The entanglement between two spins i, j in the same chain is depicted in Fig. 3 through the pair negativity $N_{ij} = (\text{Tr}|\rho_{ij}^{\text{pt}}| - 1)/2$ [62], where ρ_{ij}^{pt} is the partial transpose of ρ_{ij} . N_{ij} exhibits a stepwise behavior, reflecting the magnetization plateaus, with the onset of entanglement determined precisely by the FFs and that of the $|M| = Ns - 1$ plateau [Eq. (15)]. Because of the interplay between fields and exchange couplings, N_{ij} increases for decreasing $|M|$ for contiguous pairs (top left), since the spins become less aligned, but shows an asymmetric behavior for second neighbors (top right), as these pairs become more aligned when M increases and acquires the same sign as the corresponding field. Third neighbors (bottom left) remain appreciably entangled at the FFs, since there $N_{14} = N_{12} = N_{oe}$. This property also holds at the border (15) due to the W -like structure of the $M = Ns - 1$ GS (see Supplemental Material [57] for expressions of N_{ij} and the concurrence). The exact negativities at factorization in the projected states (11) (bottom right), obtained from (14), exhibit the same previous behavior with M for any s . They are in compliance with the monogamy property, decreasing as N^{-1} for large N at fixed finite M .

The general picture for other field configurations is similar, but differences do arise, as shown in Fig. 4. While in all cases the $|M| < Ns$ plateaus emerge from the FFs, with the diagram of the alternating square lattice

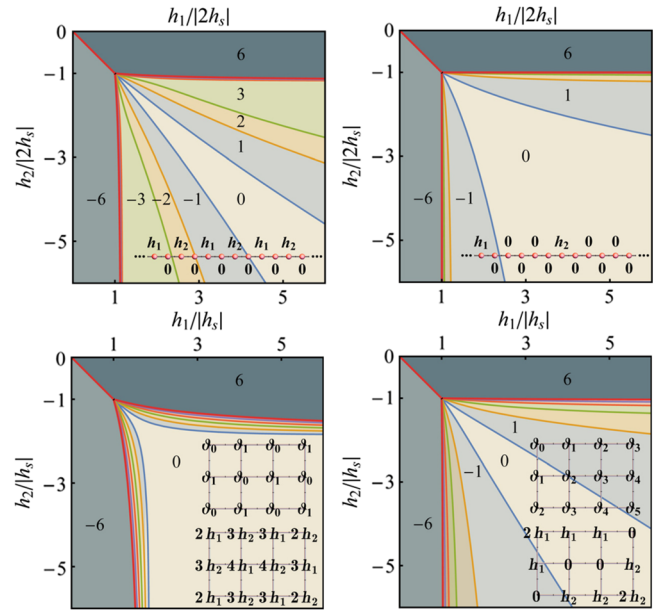


FIG. 4. Exact GS magnetization diagram for distinct spin arrays and field configurations with $\Delta = 1.2$. Top: Cyclic $N = 12$ spin-1/2 chain with next alternating fields (left) and a zero-bulk field (right). Bottom: Open 3×4 spin-1/2 arrays with alternating (left) and zero-bulk (right) field configurations. All plateaus merge at the factorizing point, where the GS has the indicated angles. Field-induced frustration in configurations with zero fields leads to a reduced $M = 0$ plateau.

remaining similar to that of Fig. 2, the chain with next alternating fields ($h_1, 0, h_2, 0, \dots$) exhibits a much reduced $M = 0$ plateau and wider sectors with finite $|M| \leq N_S/2$. This effect is due to the intermediate spins with zero field, which are frustrated for $M = 0$ (field-induced frustration) and become more rapidly aligned with the stronger field as it increases, and facilitates the selection through nonuniform fields of different magnetizations. A similar, though attenuated, effect occurs in the zero-bulk field configurations (right panels). Moreover, in these three cases, selected pairs of spins with zero field can remain significantly entangled in the $M = 0$ plateau for strong h_1 and h_2 of opposite signs, as shown in Supplemental Material [57]. The definite M states at factorization become more complex, leading to several distinct reduced pair states, whose negativities become maximum at different M values [57].

We have proved the existence of a whole family of completely separable symmetry-breaking exact GSs in arrays of general spins with XXZ couplings, which arise for a wide range of nonuniform field configurations of zero sum [Eq. (9)]. They correspond to a multicritical point where all GS magnetization plateaus coalesce and where entanglement reaches full range for all nonaligned definite- M GSs. This point can arise even for simple field architectures, like just two nonzero edge fields of opposite sign in a chain or edge fields in a lattice, and for any size $N \geq 2$ and spin $s \geq 1/2$. Different GS magnetization diagrams can be generated, opening the possibility to access distinct types of GSs (from separable with arbitrary spin orientation at one site to entangled with any $|M| < S$) with small field variations and, hence, to engineer specific GSs useful for quantum processing tasks. Recent tunable realizations of finite XXZ arrays [28,29,41] (see also Supplemental Material [57]) provide a promising scenario for applying these results.

The authors acknowledge support from CONICET (M. C. and N. C.) and CIC (R. R.) of Argentina. This work was supported by CONICET PIP 11220150100732.

[1] J. Kurmann, H. Thomas, and G. Müller, *Physica A (Amsterdam)* **112**, 235 (1982).
 [2] G. Müller and R. E. Shrock, *Phys. Rev. B* **32**, 5845 (1985).
 [3] T. Roscilde, P. Verrucchi, A. Fubini, S. Haas, and V. Tognetti, *Phys. Rev. Lett.* **93**, 167203 (2004); **94**, 147208 (2005).
 [4] L. Amico, F. Baroni, A. Fubini, D. Patane, V. Tognetti, and P. Verrucchi, *Phys. Rev. A* **74**, 022322 (2006); F. Baroni, A. Fubini, V. Tognetti, and P. Verrucchi, *J. Phys. A* **40**, 9845 (2007).
 [5] F. Franchini, A. R. Its, B-Q. Jin, and V. E. Korepin, *J. Phys. A* **40**, 8467 (2007).
 [6] S. M. Giampaolo, F. Illuminati, P. Verrucchi, and S. De Siena, *Phys. Rev. A* **77**, 012319 (2008).
 [7] S. M. Giampaolo, G. Adesso, and F. Illuminati, *Phys. Rev. Lett.* **100**, 197201 (2008); *Phys. Rev. B* **79**, 224434 (2009); *Phys. Rev. Lett.* **104**, 207202 (2010).

[8] R. Rossignoli, N. Canosa, and J. M. Matera, *Phys. Rev. A* **77**, 052322 (2008); **80**, 062325 (2009).
 [9] N. Canosa, R. Rossignoli, and J. M. Matera, *Phys. Rev. B* **81**, 054415 (2010); L. Ciliberti, R. Rossignoli, and N. Canosa, *Phys. Rev. A* **82**, 042316 (2010).
 [10] G. L. Giorgi, *Phys. Rev. B* **79**, 060405(R) (2009); B. Tomasello, D. Rossini, A. Hamma, and L. Amico, *Europhys. Lett.* **96**, 27002 (2011).
 [11] M. Rezai, A. Langari, and J. Abouie, *Phys. Rev. B* **81**, 060401(R) (2010); J. Abouie, A. Langari, and M. Siahhatgar, *J. Phys. Condens. Matter* **22**, 216008 (2010).
 [12] S. Campbell, J. Richens, N. L. Gullo, and T. Busch, *Phys. Rev. A* **88**, 062305 (2013); G. Karpat, B. Cakmak, and F. F. Fanchini, *Phys. Rev. B* **90**, 104431 (2014); T. Chanda, T. Das, D. Sadhukhan, A. K. Pal, A. Sen De, and U. Sen, *Phys. Rev. A* **94**, 042310 (2016); S. Dusuel and J. Vidal, *Phys. Rev. B* **71**, 224420 (2005).
 [13] M. Cerezo, R. Rossignoli, and N. Canosa, *Phys. Rev. B* **92**, 224422 (2015); *Phys. Rev. A* **94**, 042335 (2016).
 [14] H. Bethe, *Z. Phys.* **71**, 205 (1931).
 [15] R. J. Baxter, *Exactly Solved Models in Statistical Mechanics* (Academic, New York, 1982).
 [16] M. Takahashi, *Thermodynamics of One-Dimensional Solvable Models* (Cambridge University Press, Cambridge, England, 1999).
 [17] S. Sachdev, *Quantum Phase Transitions* (Cambridge University Press, Cambridge, England, 1999).
 [18] C. N. Yang and C. P. Yang, *Phys. Rev.* **150**, 321 (1966).
 [19] J. D. Johnson and M. McCoy, *Phys. Rev. A* **6**, 1613 (1972).
 [20] F. C. Alcaraz and A. L. Malvezzi, *J. Phys. A* **28**, 1521 (1995).
 [21] D. V. Dmitriev and V. Ya. Krivnov, *Phys. Rev. B* **70**, 144414 (2004).
 [22] N. Canosa and R. Rossignoli, *Phys. Rev. A* **73**, 022347 (2006); E. Ríos, R. Rossignoli, and N. Canosa, *J. Phys. B* **50**, 095501 (2017).
 [23] O. Breunig, M. Garst, E. Sela, B. Buldmann, P. Becker, L. Bohatý, R. Müller, and T. Lorenz, *Phys. Rev. Lett.* **111**, 187202 (2013).
 [24] D. Giuliano, D. Rossini, P. Sodano, and A. Trombettoni, *Phys. Rev. B* **87**, 035104 (2013).
 [25] M. T. Thomaz, E. V. Correa Silva, and O. Rojas, *Condens. Matter Phys.* **17**, 23002 (2014).
 [26] R. G. Melko, *J. Phys. Condens. Matter* **19**, 145203 (2007).
 [27] M. Lewenstein, A. Sanpera, and V. Ahufinger, *Ultracold Atoms in Optical Lattices: Simulating Quantum Many-Body Systems* (Oxford University Press, New York, 2012).
 [28] O. V. Marchukov, A. G. Volosniev, M. Valiente, D. Petrosyan, and N. T. Zinner, *Nat. Commun.* **7**, 13070 (2016); A. G. Volosniev, D. Petrosyan, M. Valiente, D. V. Fedorov, A. S. Jensen, and N. T. Zinner, *Phys. Rev. A* **91**, 023620 (2015).
 [29] T. L. Nguyen *et al.*, [arXiv:1707.04397](https://arxiv.org/abs/1707.04397).
 [30] I. M. Georgescu, S. Ashhab, and F. Nori, *Rev. Mod. Phys.* **86**, 153 (2014).
 [31] *Principles and Methods of Quantum Information Technologies*, edited by Y. Yamamoto and K. Semba (Springer, New York, 2016).
 [32] L. M. Duan, E. Demler, and M. D. Lukin, *Phys. Rev. Lett.* **91**, 090402 (2003).
 [33] K. Kim, M. S. Chang, R. Islam, S. Korenblit, L. M. Duan, and C. Monroe, *Phys. Rev. Lett.* **103**, 120502 (2009).

- [34] T. Fukuhara, P. Schauß, M. Endres, S. Hild, M. Cheneau, I. Bloch, and C. Gross, *Nature (London)* **502**, 76 (2013).
- [35] C. Noh and D. G. Angelakis, *Rep. Prog. Phys.* **80**, 016401 (2017).
- [36] Z. X. Chen, Z. W. Zhou, X. Zhou, X. F. Zhou, and G. C. Guo, *Phys. Rev. A* **81**, 022303 (2010).
- [37] M. J. Hartmann, F. G. S. L. Brandao, and M. B. Plenio, *Phys. Rev. Lett.* **99**, 160501 (2007).
- [38] Y. Salathé *et al.*, *Phys. Rev. X* **5**, 021027 (2015).
- [39] G. Wendin, *Rep. Prog. Phys.* **80**, 106001 (2017).
- [40] R. Barends *et al.*, *Nature (London)* **534**, 222 (2016); *Phys. Rev. Lett.* **111**, 080502 (2013).
- [41] G. Xu and G. Long, *Sci. Rep.* **4**, 6814 (2014).
- [42] M. H. Devoret and R. J. Schoelkopf, *Science* **339**, 1169 (2013).
- [43] D. Porras and J. I. Cirac, *Phys. Rev. Lett.* **92**, 207901 (2004).
- [44] R. Blatt and C. F. Roos, *Nat. Phys.* **8**, 277 (2012).
- [45] S. Korenblit *et al.*, *New J. Phys.* **14**, 095024 (2012).
- [46] I. Arrazola, J. S. Pedernales, L. Lamata, and E. Solano, *Sci. Rep.* **6**, 30534 (2016).
- [47] R. Toskovic, R. van den Berg, A. Spinelli, I. S. Eliens, B. van den Toorn, B. Bryant, J.-S. Caux, and A. F. Otte, *Nat. Phys.* **12**, 656 (2016).
- [48] Y. P. Shim, S. Oh, X. Hu, and M. Friesen, *Phys. Rev. Lett.* **106**, 180503 (2011).
- [49] D. Loss and D. P. DiVincenzo, *Phys. Rev. A* **57**, 120 (1998).
- [50] B. E. Kane, *Nature (London)* **393**, 133 (1998).
- [51] S. C. Benjamin and S. Bose, *Phys. Rev. A* **70**, 032314 (2004); *Phys. Rev. Lett.* **90**, 247901 (2003).
- [52] J. L. Guo, J. Nie, and H. S. Song, *Commun. Theor. Phys.* **49**, 1435 (2008).
- [53] A. Bayat and S. Bose, *Phys. Rev. A* **81**, 012304 (2010).
- [54] L. Bianchi, A. Bayat, P. Verrucchi, and S. Bose, *Phys. Rev. Lett.* **106**, 140501 (2011).
- [55] Q. Chen, J. Cheng, K. L. Wang, and J. Du, *Phys. Rev. A* **74**, 034303 (2006); Y. Wan-Li, W. Hua, F. Mang, and A. Jun-Hong, *Chin. Phys. B* **18**, 3677 (2009); D. Türkpençe, F. Altintas, M. Paternostro, and O. Müstecaplıoğlu, *Europhys. Lett.* **117**, 50002 (2017).
- [56] As $(\theta, \phi + \pi)$ is equivalent to $(-\theta, \phi)$, it is unnecessary to consider solutions with $\phi_{ij} = \pi$ [which also satisfy Eqs. (4) and (6)] if negative values of θ are allowed.
- [57] See Supplemental Material at <http://link.aps.org/supplemental/10.1103/PhysRevLett.119.220605> for proofs and further elaboration of our results, which includes Refs. [58–60].
- [58] J. Ginépro and T. C. Hull, *J. Integer Seq.* **17**, 14.10.8 (2014).
- [59] R. J. Mathar, [arXiv:1406.7788](https://arxiv.org/abs/1406.7788).
- [60] E. H. Lieb, *Phys. Rev.* **162**, 162 (1967).
- [61] $\langle S_i^z \rangle_M$ is the average at the projected states (11)–(14).
- [62] G. Vidal and R. F. Werner, *Phys. Rev. A* **65**, 032314 (2002); K. Życzkowski, P. Horodecki, A. Sanpera, and M. Lewenstein, *Phys. Rev. A* **58**, 883 (1998); K. Życzkowski, *ibid.* **60**, 3496 (1999).